Catalysis Letters Vol. 110, Nos. 1–2, August 2006 (© 2006)
DOI: 10.1007/s10562-006-0093-z

Search for confinement effects in mesoporous supports: hydrogenation of *o*-xylene on Pt°/MCM-41

Franck Letellier,[a,b] Juliette Blanchard,[a,*] Katia Fajerwerg,[a] Catherine Louis,[a] Michèle Breysse,[a] Denis Guillaume,[b] and Denis Uzio[b]

[a]*Laboratoire de Réactivité de Surface, UMR CNRS 7609, Université Paris VI Pierre et Marie Curie, 75252 Paris Cedex, France*
[b]*Institut Français du Pétrole, Direction Catalyse et Séparation, BP no 3, 69390 Vernaison Cedex, France*

Received 2 March 2006; accepted 11 April 2006

The occurrence in mesoporous supports of a confinement effect related to the adsorption strength of a reaction intermediate on a metallic phase dispersed in the mesopores is examined, as well as its effect on the activity and selectivity. A model is proposed in order to determine the catalyst requirements (size of the pores and of the metal particles), which would allow to maximise the confinement. Alkyltrimethylammonium surfactants with increasing alkyl chain length were used to prepare MCM-41 supports, with controlled pore size between 22 and 39 Å and Pt° particles of controlled size (from 11 to 18 Å) were formed in the porosity of the MCM-41 supports. The reaction of hydrogenation of *o*-xylene was chosen as model reaction, because (i) previous studies have highlighted the influence of the adsorption strength of 1,2-dimethylcyclohexene (DMCHE, reaction intermediate formed by *cis*-addition of four hydrogen atoms on *o*-xylene) on the metallic surface on the selectivity toward *trans*-dimethylcyclohexane (*trans*-DMCH) and (ii) the kinetic diameter of DMCHE (6.4 Å) is close to the distance between the metallic particle surface and the silica wall of the series of Pt°/MCM-41 catalysts. Slight decrease in the turn-over frequency (TOF) and increase in the selectivity toward *trans*-DMCH are observed for the smaller pore sizes, and the assignment of this effect to a confinement of the reaction intermediate is discussed.

KEY WORDS: confinement; mesoporous; MCM-41; *o*-xylene; hydrogenation; pore size.

1. Introduction

In the field of catalysis, the term confinement covers a wide range of phenomena such as the controlled growth of metal or oxide nanoparticles in the spatially constrained space defined by the porosity of the support [1,2], the conformational constraint imposed by this same space to reactant molecules and/or chiral catalysts (with applications in the field of enantioselective catalysis) [3–9], the electronic confinement [10,11], or the capillary condensation of the reactant in the porosity of the support [12–15]. Among those phenomena, the confinement effect we address in this paper is related to the influence of the pore size of the support on the strength of adsorption of the reaction intermediate on the active phase, and in turn on the activity and/or selectivity of the catalyst. This effect was first discovered by Derouane *et al.* [16,17], who showed that up to 40% of the heat of adsorption of simple amines in the porosity of zeolite (MFI, MOR) could be assigned to confinements effects. Van der Waals interactions between the organic molecule and the zeolite framework would be responsible for this effect, and would account for the high acidity of zeolites compared to amorphous silica–alumina supports.

*To whom correspondence should be addressed.
E-mail: jblanch@ccr.jussieu.fr

This kind of confinement effect has, however, not yet been studied in the porosity of mesoporous supports, because the pore size of these supports is, except for very bulky reactants [18], usually much too large to allow the observation of such effect. However, when a more complex system is considered, composed of a nanoparticle of active phase in a cylindrical pore, the residual space between the nanoparticle surface and the silica wall can be close to the size of a simple organic molecule (see figure 1a). The purpose of this study is to determine whether an effect of the pore size on the strength of adsorption of the reactant on the active phase may exist in such systems.

One of the difficulties of these systems is that only a fraction of the nanoparticle surface is close enough to the cavity to induce the confinement of the adsorbed reactant (see figure 1). It is therefore necessary to determine, depending on the pore and metallic particle sizes, the fraction of the surface of active phase, which can confine the reactant. A model was developed for this purpose and is presented in the first part of this paper. This model was also used to determine the catalysts characteristics (pore size of the support, particle size of the active phase) that would permit the observation of a confinement effect. This study necessitates also the choice of an appropriate catalytic reaction. The reasons for the choice of the reaction of hydrogenation of *o*-xylene to *cis*- and

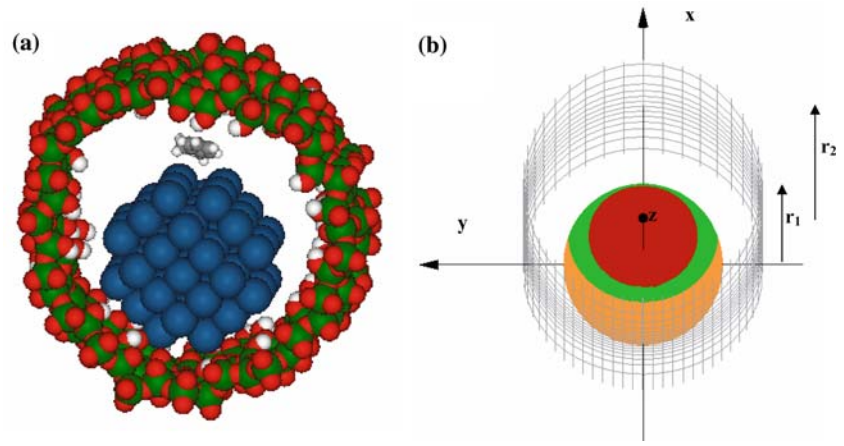

Figure 1. (a) Picture representing the confinement of DMCHE adsorbed on the Pt particle surface (d_2 = 20 Å), the Pt particle is located in a tubular pore of a MCM-41 (d_1 = 30 Å); (b) model of confinement for a particle of 2 nm in a pore of 3 nm (grey grid). The light (orange) surface corresponds to the part of the particle which is too close to the silica wall, the medium (green) surface corresponds to the part of the surface where adsorbed reaction intermediate is confined and the dark (red) surface correspond to the part of the surface which is too far to the silica wall to undergo confinement.

trans-dimethylcyclohexane (*cis*-DMCH and *trans*-DMCH) are explained in the second part.

A careful control of both the particle size and the pore size is of importance in order to study this confinement effect. The samples used for this study are therefore Pt°/MCM-41 catalysts with controlled and adjustable pore size and similar Pt° particle size. The pore size of MCM-41 supports was varied by changing the synthesis conditions (length of the alkyl chain of the surfactant, calcination temperature, and Pt° nanoparticles of controlled size (~15 Å) were formed in their porosity by ion-exchange of $[Pt(NH_3)_4]^{2+}$ at pH = 8 followed by washing, calcination and reduction. The characteristics of the MCM-41 supports and of the Pt°/MCM-41 catalysts are presented in the third part.

In the fourth part, the modification of the selectivities and activities of the Pt/MCM-41 catalysts as a function of the pore sizes of the MCM-41 support are presented and compared to those of Pt catalysts supported on a non-porous silica (areosil 380). The assignment of these modifications to a confinement of the reaction intermediate (1,2-dimethylcyclohexene, noted DMCHE) is finally discussed.

2. Experimental

2.1. MCM-41 synthesis

MCM-41 supports were prepared according to the procedure developed by Ryoo and coworkers [19], which leads to a high condensation of the silica walls and ensures therefore an optimum stability for the mesoporous supports. The pore size was varied through the use of surfactants of various chain lengths, namely octyl (C_8)-, dodecyl (C_{12})-, hexadecyl (C_{16})-trimethylammonium chloride and decyl (C_{10})-trimethylammonium bromide (Fluka). The molar ratios of the precursors were the same for all the syntheses: $4SiO_2/1Na_2O/1C_xTMA/400H_2O/3NaCl$ (where C_xTMA is an alkyltrimethylammonium, and x is the number of carbons in the alkyl chain, x = 8, 10, 12, 16). Ludox HS40 colloidal silica (Aldrich) was used as SiO_2 source. The surfactant was removed by ion-exchange followed by calcination as described in [20]. The calcined supports were denoted C_xMCM-41 where x stands for the number of carbons in the alkyl chain of the surfactant.

2.2. Catalysts preparation

The compound used as Pt precursor was $Pt(NH_3)_4(OH)_2$ (5 wt% aqueous solution, Alfa-Johnson Mathey). C_xMCM-41 and a non-porous reference silica denoted Aero380 (Aerosil 380, Degussa, $S_{BET} \asymp 380\ m^2\ g^{-1}$) were used as supports. Pt°/C_xMCM-41, and Pt°/Aero380 samples were prepared following a procedure described by Gonzalez *et al.* [21]. This procedure, which uses the fact that the surface of silica is negatively charged above its point of zero-charge (PZC $\asymp$2 for amorphous silica), allows the adsorption on the silica surface of all the platinum ($[Pt(NH_3)_6]^{3+}$) initially present in the solution (0.4–1.5 wt% Pt on silica) and is very efficient for the preparation of highly dispersed nanoparticles on mesoporous supports [22]. The samples were prepared as described in [23]. The samples were reduced in pure H_2 ($2L\ h^{-1}\ g^{-1}$) at 573 K (rate: 2 K min^{-1}) during 2 h with an intermediate step at 423 K during 1 h.

2.3. Catalyst characterisation

The *Pt content* (wt%) in the calcined samples was measured by ICP (Central Analysis Service of the CNRS, Vernaison France).

N_2 adsorption–desorption isotherms were obtained on a Micromeritics ASAP 2010 system at 77 K. Before anal-

ysis the supports and catalysts were degassed at 423 K, under a pressure of 1 Pa for 5 h. The average pore sizes (w_d) were calculated using the DFT method and/or the geometrical model proposed by Kruk *et al.* [24].

The metal dispersion in Pt°/C_xMCM-41 was determined by H_2–O_2 pulse titration on a χ-sorb apparatus® (IFP's Licence). The sample was first reduced *in situ* under pure H_2, using the experimental conditions described in the preparation part, and the temperature was decreased to 298 K under a stream of H_2. After 10 min purge under He a titration with O_2 (5% O_2/He) was performed . The titration reaction is based on the equation (1):

$$Pt_s\text{--}H + 3/4O_2 \rightarrow Pt_s\text{--}O + 1/2H_2O, \quad (1)$$

where Pt_s stands for a Pt atom at the surface of a Pt particle.

The average Pt particle diameter d_{Pt} was deduced from the Pt dispersion (D%, H_2/O_2 titration) assuming a cubooctaedral geometry for Pt particles [25] (equation (2)).

$$d_{Pt} = \frac{6}{\rho \times S_{Pt} \times D}, \quad (2)$$

where ρ is the metallic platinum density (21.45 g cm^{-3}), S_{Pt} the surface area of metallic platinum (275 m^2 g^{-1}).

Transmission Electron Microscopy of the reduced catalysts was performed on a JEOL-TEM 100 CXII apparatus, in order to determine the Pt° particle size distribution and the average particle size. Ultramicrotomed slices were used to obtain extensive electron-transparent regions, and to ascertain that the observed particles were really located in the porosity of the mesoporous supports. The samples were prepared by embedding the catalyst in a polymer resin subsequently cured at 343 K for 2 days. Ultramicrotomed slices (ca. 70 nm thick) of the embedded sample were cut using a diamond knife, and laid on carbon-covered copper grids. In order to have an accurate comparison with chemisorption measurements, the surface-averaged particle diameter (d) was calculated from the particle size distribution (estimated from ca. 500 particles) using equation (3):

$$d = \frac{\sum n_i d_i^3}{\sum n_i d_i^2}. \quad (3)$$

2.4. Hydrogenation of o-xylene: catalytic activities and selectivities measurements

The gas composition at thermodynamic equilibrium was calculated at 383 K (operating temperature) using the thermodynamic parameters determined by Neyestanaki *et al.* [26]: *o*-xylene conversion 90%, *trans*-DMCH selectivity 50%, for [H_2]/[*o*-xylene] = 10 (molar ratio). To avoid the formation of preferential paths and transfer heat phenomena through the catalyst bed, the catalyst (0.25 g) was diluted with silicon carbide. The reaction conditions were defined in order to obtain a zero order kinetic with respect to *o*-xylene.

The absence of external diffusion limitations (diffusion from the bulk to the surface of the support crystallite) was established by varying the catalyst weight with a constant contact time. A 2-fold increase in the sample weight did not affect the conversion for a given contact time. This shows that external diffusion limitations are absent. The Weisz–Prater criterion [27] was used to detect possible internal diffusion limitations. This criterion is based on the calculation of a modulus Z_s (see equation 4)): if $Z_s \ll 1$ no internal diffusion limitations are to be considered, whatever the kinetic rate of the reaction [28–30]. This criterion is easier to use than the Thiele modulus because it contains exclusively parameters that can be observed or measured.

$$\Phi_s = \frac{r_p^2 \cdot V_s \cdot \tau}{4850 \cdot r_e^2 \cdot S_g \cdot C_s} \cdot \sqrt{\frac{M}{T}} \text{ for a spherical particle,} \quad (4)$$

where r_p is the radius of the catalyst pellet (cm), V_s the specific rate of the reaction (mol g^{-1} s^{-1}), r_e is the average pore size (cm), S_g the specific surface area (cm^2 g^{-1}), C_s the concentration of reactant in the feed (mol cm^{-3}), M the molecular weight of the reactant (g mol^{-1}), T the reaction temperature (K) and τ tortuosity factor of the pores. τ is equal to 1 in perfect cylinder, but could exceed this value when an active phase is supported in cylindrical pores, because its presence may result in constrictions in the pores. In any case, the highest possible value of τ is 10.

Prior to catalytic tests, catalysts were reduced *in situ* using the experimental conditions described in the preparation part. The test was performed in a continuous fixed-bed quartz reactor under atmospheric pressure at 383 K. The feed, 5 vol% of *o*-xylene in *n*-heptane, [H_2]/[*o*-xylene] = 10 (molar ratio), was injected by a pump and vapourised in the catalyst bed. Effluents were collected in a condenser filled with dry ice (T = 193 K), and analysed every 30 min with a "Varian 3400" gas chromatograph equipped with a 50 m length Pona column and a FID detector.

The conversions and selectivities were measured after pseudo-steady states were reached (usually 2 h time-on-stream) at two weight hour space velocity (whsv), namely 34 and 68 h^{-1}. The uncertainties of the measurements (± 2% on the conversion and ± 1% on the *trans*-DMCH selectivity) were evaluated from reproducibility tests performed on the 0.8Pt/aero380 catalyst.

3. Results

3.1. Model of confinement

According to Derouane and Chang [16], the confinement of a molecule into a zeolitic cavity arises from an increase of the heat of adsorption of this molecule,

due to attractive van der Waals interactions with the cavity framework. The model we propose in order to examine the confinement effect in a mesopore is sketched in figure 1b: a spherical particle of radius r_1 is located in a cylindrical pore of radius r_2, and the particle is covered by reactants and reaction intermediates (zero order reaction i.e. the particle surface is saturated). Among those molecules, some will undergo confinement, some not, depending on their distance from the silica wall. It is indeed commonly admitted that a molecule is confined if its size is at least 0.6 time the size of the cavity [16]. The purpose of the model is to determine what percentage of the surface of the particle (and in turn what percentage of the adsorbed reaction intermediate) is subjected to the confinement effect. In the present case, we will assume that only the molecules whose distance to the silica wall is smaller than $d_{\text{reactant}}/0.6$ undergo confinement. Moreover, we will exclude from the calculation of the molecules lying below the bottom part of the particle, and which may therefore be too close to the silica wall to be easily accessible.

The percentage of confined surface was calculated as follows: the origin of the coordinates was taken at the centre of the sphere. The equation of the cylinder in spherical coordinates is:

$$(r\sin\theta\cos\varphi + r_2 - r_1)^2 + r^2\sin^2\theta\sin^2\varphi = r_2^2. \qquad (5)$$

The distance L of the sphere surface to the cylinder being equal to $r - r_1$, the following equation is obtained:

$$\cos\varphi = \frac{\left(\frac{L}{r_1}+1\right)^2 \sin^2\theta + 1 - 2\cdot\frac{r_2}{r_1}}{2\left(\frac{L}{r_1}+1\right)\cdot\left(\frac{r_2}{r_1}-1\right)\cdot\sin\theta}.$$

In the case of $r_1 = 1$ nm and 1.35 nm $\leq r_2 \leq$ 1.65 nm, the areas of three distinct zones of the sphere (defined below) were calculated numerically using Mathematica, by integration of the surface of the sphere($S = r_1\sin\theta\cdot d\theta\cdot d\varphi$) with equation (6) to define the limits

- $L \leq L_{\min}$, corresponds to the bottom area of the sphere (i.e. the part of the surface that might not be easily accessible to the reactant molecules);
- $L_{\min} \leq L \leq L_{\max}$, is the part of the sphere where a confinement of the adsorbed reaction intermediate can be expected;
- $L_{\max} \geq L$, is the part of the sphere, for which the adsorbed reaction intermediate are too far from the pore surface to undergo confinement.

The $L_{\max}$ (1.2 nm) and $L_{\min}$ (0.7 nm) values were evaluated using the kinetic diameter of *DMCHE* (d_{DMCHE} = 0.64 nm): $d_{\min} \asymp d_{\text{DMCHE}}$ and $d_{\max} = d_{\text{DMCHE}}/0.6$ [16].

The graphical representations and numerical calculations of these three surfaces for 1.35 nm $\leq r_2 \leq$ 1.65 nm (figure 2) show that the percentage of confined reactant is maximum for 1.4 nm $\leq r_2 \leq$ 1.5 nm and represent about 30% of the overall particle surface, which should be large enough to be detected.

3.2. Choice of o-xylene hydrogenation as model reaction

Previous studies showed that, in the reaction of *o*-xylene hydrogenation, an increase in the selectivity to *trans*-DMCH was observed upon decreasing the electron density of the metallic particle, either by increasing the acidity of the support [31,32] or by changing the nature of the metallic phase [33,34]. This effect was assigned to a stronger interaction between the metallic surface and the unsaturated hydrocarbon. The roll-over mechanism, proposed first by Inoue *et al.* [35] for

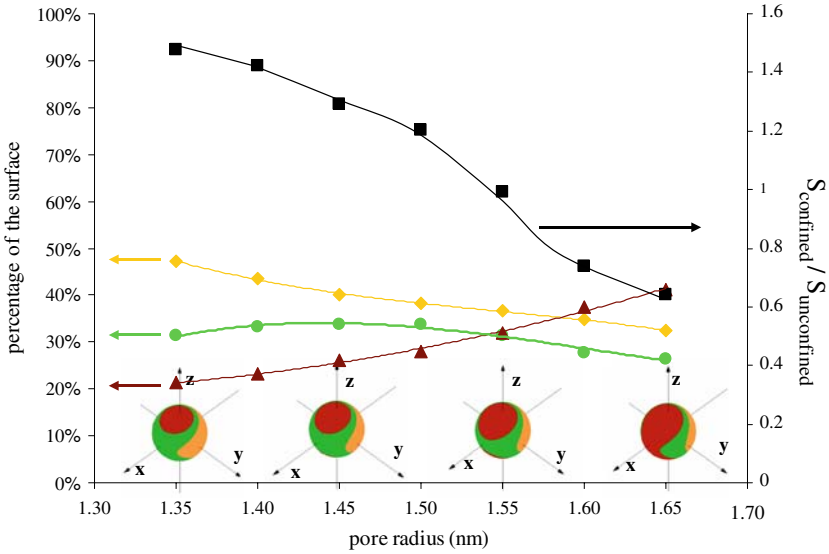

Figure 2. Calculation of the relative percentages of the three types of surfaces defined in figure 1b.

the isotopic exchange of cyclopentane, was proposed later to explain the selectivity of the *o*-xylene hydrogenation reaction [26,32,36,37]. It accounts well for the observed modification of the selectivity with the electronic density of the metallic phase: after fast adsorption of *o*-xylene and *cis*-addition of four hydrogen atoms, adsorbed 1,2-dimethylcyclohexene (1,2-DMCHE) is formed, and partly isomerised to 2,3-DMCHE. The latter is either directly hydrogenated, leading to the formation of *cis*-DMCH, or rolls over on the opposite side of its aromatic ring, leading, after hydrogenation, to *trans*-DMCH. According to this model, the rate of formation of *trans*-DMCH is determined by the relative rates of hydrogenation and isomerisation of 1,2-DMCHE, and therefore by adsorption strength of 1,2-DMCHE on metallic surfaces. This mechanism is still questioned and another mechanism has been more recently proposed, which involves the desorption of DMCHE and its readsorption followed by hydrogenation [38–40]. This alternative mechanism also accounts for the influence of the adsorption strength of DMCHE on the *cis*/*trans* selectivity. Moreover a higher heat of adsorption may also result in a decrease of activity (Sabatier Principle). Guillon *et al.* [34] observed for example dramatic changes in the activity and in the selectivity, when the metallic properties varied, upon changing the composition of the bimetallic phase for the reaction of hydrogenation of *o*-xylene over bimetallic PtPd and PtGe catalysts supported on alumina. In the present paper, any electronic effect of the support [33] can be discarded, as it is well known that pure silica is a non-acidic support. The confinement effect we address being related to a modification in the adsorption strength of DMCHE, a decrease in the activity and/or an increase in the *trans*-selectivity are expected when the size of the reactant matches the size of the cavity formed between the metallic particle surface and the silica wall.

3.3. Characterisation of the C_xMCM-41 supports and $Pt°/C_x$MCM-41 catalysts

3.3.1. Characterisation of the support before and after introduction of Pt

The synthesis procedure we applied for the preparation of C_xMCM-41 was initially developed for the preparation of C_{16}MCM-41 [19]. We checked, using XRD (result not shown) that the MCM-41 structure was preserved upon replacing $C_{16}TMA^+$, by C_{12}, C_{10} or C_8TMA^+. However, whereas C_{16}MCM-41 and C_{12}MCM-41 possess ordered hexagonal structures with well defined (100), (110) and (200) peaks, the intensities of these three peaks were much smaller for C_{10}MCM-41, and only one weak and broad peak corresponding to (100) was observed for C_8MCM-41. This reveals a less ordered structure for the MCM-41 prepared with the shorter surfactant chains. A shift in the position of the (100) peak toward larger angles upon decreasing the chain length of the surfactant is also clearly visible, indicating a decrease in the d-spacing of the hexagonal structure (table 1).

The sorption isotherms of C_{16}MCM41 and C_{12}MCM-41 (figure 3, curves (a) and (b)) are characteristic of ordered mesoporous supports (IUPAC type IV isotherm) with a steep N_2 uptake at $P/P^0 = 0.35$ and 0.25, respectively, whereas the sorption isotherms of the two other samples (figure 3 curves (c) and (d)) were characteristic of supermicroporous materials (pore size around 20 Å). BJH method being inadequate for materials having pore size smaller than 20 Å, the geometrical model proposed by Kruk *et al.* [24] and the DFT method were used to calculate the average pore size w_d (table 1) and the pore size distribution was calculated using the DFT method (figure 4). The average pore sizes calculated using the geometrical model are between 2 and 6 Å larger than the pore size calculated using DFT, but they follow the same trend with the surfactant chain length. A decrease of 16 Å in the pore diameter is observed upon

Table 1
Structural features of MCM-41 supports synthesised with decreasing surfactant chain length

MCM-41	d_{100} (Å)	V_p (cm^3/g)[a]	BET surface ($m^2\ g^{-1}$)[b]	w_d (Å)[c]
C_{16}MCM-41	40.6	0.94	1063	40 (34)
1.2Pt/C_{16}MCM-41	39.9	0.79	939 (−12%)	39
C_{12} MCM-41	34.0	0.70	1020	32 (27)
1.0Pt/C_{12}MCM-41	33.5	0.63	953 (−7%)	31
C_{10}MCM-41	30.3	0.59	1049	27 (24)
0.7Pt/C_{10}MCM-41	29.5	0.56	898 (−14%)	26
C_{10}MCM-41(1223 K)	28.2	0.32	668	22 (20)
0.8Pt/C_{10}MCM-41(1223 K)	28.0	0.31	640 (−4%)	22
C_8MCM-41	28.5	0.45	960	24 (20)
0.8Pt/C_8MCM-41	28.2	0.35	727 (−24%)	23
Aero380	–	–	350	–
0.4%Pt/Aero380	–	–	281 (−20%)	(> 80)

[a] V_p calculated at $P/P_0 = 0.9$.
[b] The value between parentheses is the variation of the surface area after introduction of Pt.
[c] w_d was calculated according to [24] and/or using the DFT model (value between parentheses).

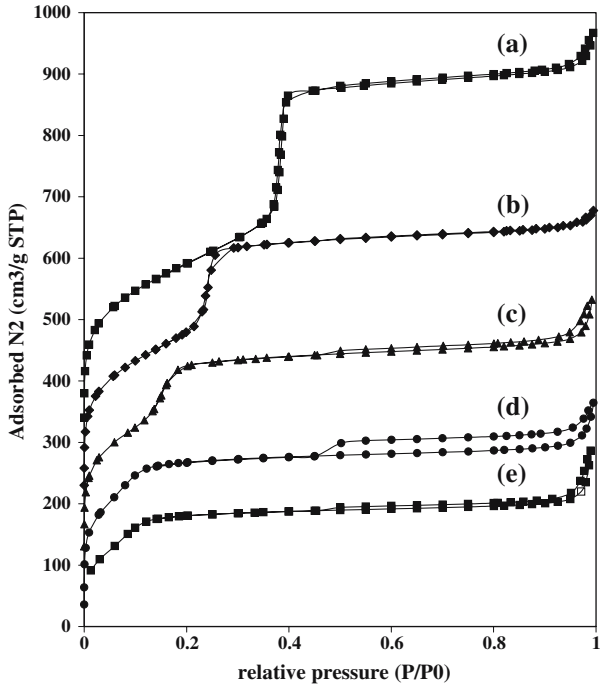

Figure 3. N_2 sorption isotherms of MCM-41 samples: (a) C_{16}MCM-41; (b) C_{12}MCM-41; (c) C_{10}MCM-41; (d) C_8MCM-41; (e) C_{10}MCM-41(1223 K) (an offset 100 $cm^3\ g^{-1}$ has been inserted between each curve).

reducing the surfactant chain length from C_{16} to C_8, in agreement with the work of Kruk *et al.* [41]. Moreover, the narrow pore size distributions and high surface areas

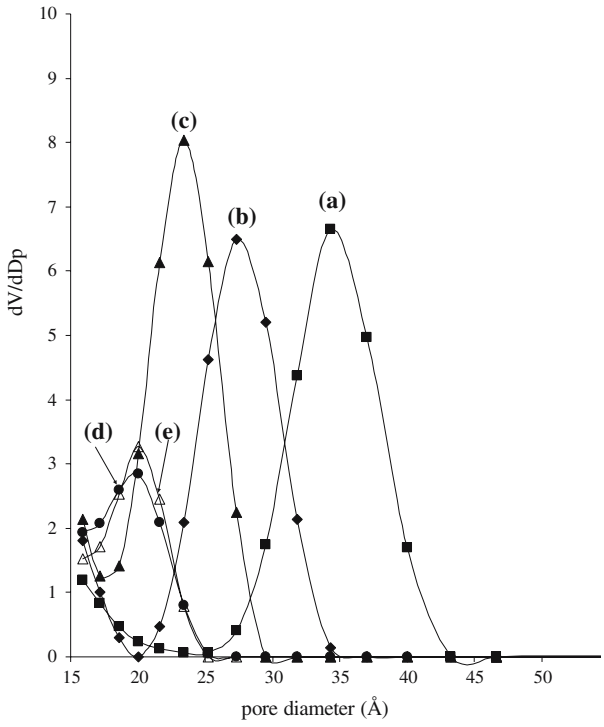

Figure 4. Pore size distribution (DFT method) of MCM-41 samples synthesised with (a) C_{16}MCM-41; (b) C_{12}MCM-41; (c) C_{10}MCM-41; (d) C_8MCM-41; (e) C_{10}MCM-41(1223 K).

of the four samples confirm the possibility to prepare high surface area MCM-41 supports with reduced pore size and controlled porosity. The decreased intensity of the XRD peaks characteristic of the hexagonal P6mm structure observed with C_{10}TMA and C_8TMA surfactants might therefore be assigned to a wormhole-like structure with controlled pore size, and does not impede the use of these supports for our study.

Calcination at high temperature is known to result in a contraction of the MCM-41 structure and has therefore been used to decrease further the pore sizes of one of the MCM-41 supports. After calcination of C_{10}MCM-41 at 1223 K instead of 823 K, a decrease of about 5 Å of the pore size was observed (see table 1), without any significant loss in the hexagonal structure (XRD, not shown).

A careful control of the pore size of the catalyst is one of the requirements imposed by the model presented in section 3.1. It is therefore of importance to ascertain that the structure of the support has not been altered upon introduction of platinum. After introduction of platinum, a slight decrease in the intensity of all the XRD lines was observed (results not shown) associated with a slight decrease in the pore volumes and surface areas (see table 1). These changes, which indicate a limited alteration of the structure upon introduction of platinum, remain, however, moderate for all the catalysts indicating that the MCM-41 structure is not significantly damaged.

Aerosil 380, a non-porous pure silica support, was used for the preparation of reference catalysts, for which no confinement was expected. It was therefore essential to establish that no porosity was generated upon introduction of Pt. The sorption isotherms of 0.4Pt/aero380 (results not shown), indicate the formation of a new porosity, probably due to some sticking between the silica particles during insertion of Pt. However, the pore size of the resulting porosity is large compared to the kinetic diameter of DMCHE: more than 90% of the pore volume can be assigned to pores larger than 100 Å. The confinement of the reaction intermediate in these catalysts can therefore be neglected.

3.3.2. Size of the Pt nanoparticles

An accurate control of the average platinum particle size and of the particle size distribution is required for the study of confinement effect. The size of the Pt° nanoparticles was evaluated using both chemisorption and electron microscopy (table 2). Using TEM on thin sections of the sample, we have been able to ascertain that the particles observed on the TEM micrographs were isolated and dispersed in the porosity of the support. The size of the Pt° particle being close to 15 Å (i.e. close to 10 Å, the limit of detection of TEM), it has not always been possible to detect enough particles to allow the determination of the particle size distribution. The average particle size determined by chemisorption and

TEM are reported in table 2. The dispersion of the Pt° phase is high, whatever the support, confirming that the synthesis method used is well-suited for the preparation of small Pt° nanoparticles. For all catalysts, the particle size distributions determined from the TEM micrographs are narrow (with more than 70% of the particles having their size in a 5 Å interval) and centred at 15 Å, and the average particle size is 17 ± 3 Å. These values are consistent with the average particle size determined by chemisorption (15 ± 4 Å). The values obtained by chemisorption and TEM are rather different for Pt°/C_8MCM-41 and Pt°/C_{10}MCM-41 for which very high dispersions (close to 100%) were measured by chemisorption. The very small size of the Pt° nanoparticles on these catalysts might be at the origin of this difference.

3.4. Hydrogenation of o-xylene

The reaction of hydrogenation of *o*-xylene on noble metals (Pt°, Pd°), which leads to the formation of two isomers, the *cis*-dimethylcyclohexane (*cis*-DMCH, kinetic isomer) and *trans*-dimethylcyclohexane (*trans*-DMCH, thermodynamic isomer), is well-suited for this study. Indeed, the size of *o*-xylene (kinetic diameter 6.4 Å) is close to the size of the residual space for a particle of 20 Å in a pore of 20–30 Å, and the reaction is zero-order with respect to *o*-xylene under our experimental conditions (T = 383 K, P_{ox} = 0.04 atm).

The Pt/C_xMCM-41 and Pt/Aero380 catalysts were tested in the reaction of hydrogenation of *o*-xylene. The conversion and selectivity values are reported in table 3. Pt/Aero380 catalysts were used to determine the variation of the selectivity versus conversion in samples where no confinement was expected. For these catalysts, a linear increase in the selectivity to *trans*-DMCH with *o*-xylene conversion was observed, (reference line in figure 5). This increase is rather moderate (less than 5% over a wide range of conversions), in agreement with previous studies, which have stated that the selectivity to *trans*-DMCH is independent of conversion within small (ca. 5%) conversion ranges [34]. Besides, a constant value of the turn over frequency (TOF = 0.06 ± 0.01 s^{-1}) was obtained for the three reference catalysts, despite variations in the dispersion of the Pt° phase and in the Pt loading (table 2). This result confirms that *o*-xylene hydrogenation over Pt/SiO_2 catalysts is a structure insensitive reaction.

The selectivities versus conversion data of Pt/C_xMCM-41 catalysts have thereafter been compared to the reference straight line (table 3 and figure 5). For Pt/C_{16}MCM-41, Pt/C_{12}MCM-41 and Pt/C_{10}MCM-41(823 K) the data are close to the reference straight line and within the experimental error. However, for the two catalysts having the smaller pore diameters (that is Pt/C_8MCM-41 and Pt/C_{10}MCM-41(1223 K)) the data are located above this straight line outside the experimental error. Furthermore, whereas the TOF of the first three samples is close to that of reference catalysts (0.06 ± 0.01 s^{-1}), it is much lower for Pt/C_8MCM-41 (0.03 s^{-1}) and slightly lower for Pt/C_{10}MCM-41(1223 K)) (0.05 s^{-1}).

4. Discussion

The purpose of this discussion is to determine whether the effects we observed on the *o*-xylene hydrogenation selectivity and activity upon decreasing the pore diameter of the catalyst can be unambiguously assigned to a confinement effect. As stated by Derouane [17] in the case of zeolites, the confinement of an organic molecule is due to its enhanced interaction with the pore-framework, leading to a higher heat of adsorption. The slightly higher selectivity to *trans*-DMCH, observed for Pt/C_8MCM-41 and Pt/C_{10}MCM-41(1223) (table 3), is therefore in agreement with a confinement effect related to a higher heat of adsorption, and so does the decreased activity in agreement with the Sabatier principle. Although there is a distribution in pore sizes and Pt° particle diameters in the real catalysts, one can use the model of confinement described above in section 3.1 for a qualitative comparison of the five mesoporous catalysts. The calculations are reported in table 4, and

Table 2
Pt/SiO_2 catalysts dispersion and average particle size determined by TEM and chemisorption

Pt/SiO_2 samples	Pt (wt%)	Dispersion (%) H_2/O_2	$d_{particle}$ (Å) H_2/O_2	$d_{particle}$ (Å) TEM[a]
0.4Pt°/Aero380	0.40	58	19	[c]
0.8Pt°/Aero380	0.79	57	19	17
1.5Pt°/Aero380	1.55	73	14	20
1.2Pt°/C_{16}MCM-41	1.2	67	15	[c]
1.0Pt°/C_{12}MCM-41	0.95	59	18	21
0.7Pt°/C_{10}MCM-41(823)	0.74	91	11	18
0.8Pt°/C_{10}MCM-41(1223)	0.81	78	13	19
0.8Pt°/C_8MCM-41	0.78	95	11	17

[a]Surface-averaged diameter (equation (3)).
[b]$d_1 = w_d$ (geometrical model, see table 1); $d_2 = d_{particle}$ H_2/O_2.
[c]Not determined.

Table 3
Activities and *trans*-DMCH selectivities of Pt/SiO_2 samples tested in *o*-xylene hydrogenation

	whsv (h^{-1})	Conversion (%)	*trans*-DMCH selectivity (%)	TOF (s^{-1})[a]
0.4Pt°/Aero380	34	11	34	0.05
	17	24.5	36	0.06
0.8Pt°/Aero380	68	12	34	0.06
	34	23	35	0.06
1.5Pt°/Aero380	68	32	36	0.06
	34	59	38	0.06
1.2Pt°/C_{16}MCM-41	68	20.5	34	0.06
	34	38	35.5	0.05
1.0Pt°/C_{12}MCM-41	34	38	35	0.07
0.7Pt°/C_{10}MCM-41	68	21	35	0.07
	34	37	36.5	0.06
0.8Pt°/C_{10}MCM-41(1223 K)	68	15	37	0.05
	34	26	39	0.05
0.8Pt°/C_8MCM-41	68	8	36	0.03
	34	20	39	0.03

T = 383 K, P = 1 atm, 5% *o*-x/*n*-C_7 vol., $[H_2]/[o\text{-xylene}]$ = 10 molar ratio, $m_{catalyst}$ = 0.25 g, whsv = 68 and 34 h^{-1}, t = 120 min.
[a]TOF was calculated using the Pt° dispersion determined by chemisorption.

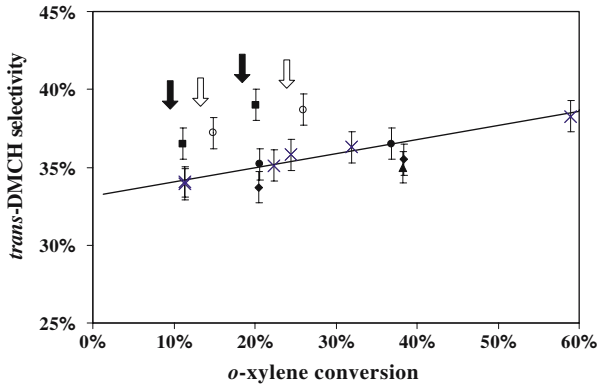

Figure 5. *trans*-DMCH selectivity as a function of *o*-xylene conversion for Pt/SiO_2 samples. (Test conditions: T = 383 K, P = 1 atm, 5% *o*-x/*n*-C_7 vol., $[H_2]/6[o\text{-xylene}]$ = 10 molar ratio, $m_{catalyst}$ = 0.25 g, whsv = 68 and 34 h^{-1}, t = 120 min)., reference Pt/aero380 catalysts; ◆, 1.2Pt/C_{16}MCM-41; ▲, 1.0Pt/C_{12}MCM-41; ●, 0.7Pt/C_{10}MCM-41; ○, 0.8Pt/C_{10}MCM-41(1223); ■, 0.8Pt/C_8MCM-41.

the ratios of the confined surface over the unconfined one are consistent with the modifications in activity and selectivity observed for Pt/C_8MCM-41 and Pt/C_{10}MCM-41(1223). Indeed, the ratio is close or higher than 1 for these two catalysts, whereas it is below 0.5 for the three other catalysts, indicating that a confinement effect can be expected for the two first catalysts only. Our results are therefore consistent with these expectations.

One can note that the changes of TOF and selectivity observed for the Pt/C_8MCM-41 and Pt°/C_{10}MCM-41(1123) (table 3 and figure 5) are rather weak compared to the decrease in *o*-xylene hydrogenation activity and selectivity reported by Guillon *et al.* [34] for metallic catalysts subjected to a modification of the electronic properties of the active phase: these authors reported a considerable variation in *trans*-DMCH selectivity (31% for Pt/Al_2O_3, 43% for $Pt_{50}Pd_{50}/Al_2O_3$, and 69% for Pd/Al_2O_3) and in the hydrogenation activity (230 mmol h^{-1} g^{-1} for Pt/Al_2O_3, 10 mmol h^{-1} g^{-1} for $Pt_{50}Pd_{50}/Al_2O_3$, and 4 mmol h^{-1} g^{-1} for Pd/Al_2O_3). In our case, the weak variation in TOF and selectivity may be due to the fact that only a fraction of the adsorbed reaction intermediate is subjected to a confinement effect (ca. 30%, see table 4) and that the TOF is the average value of the TOFs of the confined and non-confined sites while the selectivity is a TOF-weighted average (i.e. the average of the selectivities of the confined sites and non-confined sites weighted by their respective TOF).

The modification of selectivity and TOF observed for Pt/C_8MCM-41 and Pt°/C_{10}MCM-41(1223 K) being rather weak, they could as well be assigned to other causes: an electronic effect of the support and/or the formation of coke during the catalytic test (the values reported in table 3 were obtained after 2 h time-on-stream). Mass transfer limitations occurring in the narrower pores could also account for the observed decrease in the hydrogenation activity. We will try to determine if these phenomena did occur and if their amplitude could account for the effects we observed.

To evaluate the hypothesis of mass transfer limitations, the Weisz–Prater criterion (equation (4)) was considered. The values of Z_s of some of the catalysts reported in table 5 are far below 1, so according to the charts compiled by Satterfield [29], internal diffusion can be excluded.

An electronic effect of the support on the active phase [33] can also *a priori* be discarded because silica is a non-acidic support. However, Zhao and Gates [42] have observed that the toluene hydrogenation activity of very small iridium clusters (Ir_4 and Ir_6) supported on alumina was an order of magnitude lower than that of Ir aggregates of about 50 atoms. They concluded that the

Table 4
Calculation of the relative percentage of the three types of surfaces defined in figure 1b for the five mesoporous catalysts studied

Sample	w_d (Å)	$d_{particle}$ H_2/O_2 (Å)	Unconfined (%)	Confined (%)	Unaccessible (%)	Confined/unconfined
1.2Pt°/C_{16}MCM-41	39	15	54	14	32	0.27
1.0Pt°/C_{12}MCM-41	31	18	41	21	38	0.5
0.7Pt°/C_{10}MCM-41(823)	26	11	40	19	41	0.47
0.8Pt°/C_{10}MCM-41(1223)	22	13	20	31	49	1.55
0.8Pt°/C_8MCM-41	23	11	46	28	26	0.93

"Unconfined" represents the percentage of surface that is too far from the silica wall to undergo confinement, "unaccessible" represents the percentage of surface that is too close to the silica wall to be easily accessible to the reactants and "confined" represents the percentage of confined surface.

concept of structure insensitivity in metal catalyst could not be extended straightforwardly to clusters smaller than 10 Å. As the average particle size determined by chemisorption for Pt/C_8MCM-41 and Pt°/C_{10}MCM-41(1223) is close to 10 Å, a modification of the activity related to the size of the particle could occur. However, the fact that the activity and selectivity of Pt°/C_{10}MCM-41 (for which the average Pt° particle size is close to 10 Å, see table 2) are not significantly different from those of the reference catalysts (table 3), tends to indicate that this effect does not play a significant role.

The presence of ca. 4 wt% of carbon was detected on the catalysts after test (t = ca. 4 h) in agreement with the formation of coke on the metallic surface reported by Neyestanaki *et al.* [26] for the same reaction. A moderate deactivation (≤15%) similar for all the catalysts was observed between 30 and 120 min. Deactivation did most probably occur at a larger scale during the first 30 min of reaction if one refers to Neyestanaki *et al.* [26]. Deactivation between 30 and 120 min is accompanied for all catalysts by a slight increase in the *trans*-DMCH selectivity. The variation of selectivity with deactivation seems to be more pronounced on porous (+2%) than on non-porous (+1%) catalysts, but is of the same order of magnitude as the experimental error on selectivity. We cannot exclude that the variations of selectivity were more pronounced during the initial deactivation step. However, the experimental set-up did not make possible the measurement of the initial activity and selectivity. As a consequence, it is not possible to ascertain that the effects we observed on the selectivity and activity of Pt/C_8MCM-41 and Pt°/C_{10}MCM-41(1223 K) were not due to different deactivation behaviours of these two catalysts during the first minutes of reaction.

Table 5
Calculation of Z_s/τ using equation (4) for several catalysts

	Pt/Aero380	Pt/C_{16}MCM-41	Pt/C_8MCM-41
$10^2 r_p$ (cm)[a]	1.25	0.5	0.5
whsv (h^{-1})	68	68	68
Conversion (%)	12.5	20.5	8.2
10^8 V_s (mol s^{-1} g^{-1})	142	233	93
M (g mol^{-1})	106	106	106
10^6 C_s (mol cm^3)	4.21	4.21	4.21
T (K)	383	383	383
$10^7 r_e$ (cm)	25	3.9	2.3
$10^{-6} S$ (cm^2 g^{-1})	2.8	9.4	7.3
Z_s/τ	3.2×10^{-4}	1.1×10^{-3}	1.6×10^{-3}
Z_s[b]	$< 3.2 \times 10^{-3}$	$< 1.1 \times 10^{-2}$	$< 1.6 \times 10^{-2}$

[a]The value of r_p was estimated by sieving the catalyst.
[b]τ is always ≤10.

5. Conclusion

Pt°/C_xMCM-41 with controlled pore and particle sizes were prepared. Their TOFs and selectivities in the reaction of hydrogenation of *o*-xylene were compared to those of Pt° supported on non-porous silica, in order to study the occurrence of confinement effects in the mesopores of MCM-41 materials. Slightly higher *trans*-DMCH selectivity and lower TOF were observed for Pt/C_8MCM-41 and Pt°/C_{10}MCM-41(1223 K), i.e. with the catalysts having the smaller pore size and the higher ratio of the confined surface over the unconfined one. This result is consistent with a confinement effect on the adsorbed reaction intermediate (1,2-dimethylcyclohexene), and is consistent with the model of confinement proposed in this paper. The weak amplitudes of the observed effects can be explained by the fact that only a fraction of the adsorbed reaction intermediates is close enough to the silica wall to undergo confinement, but they cannot be unambiguously assigned to a confinement effect.

As mentioned in the introduction, confinement effects in mesoporous supports is a very interesting and challenging emerging issue, and the results reported in this paper deserve to be confirmed. Moreover, the confinement effect we have addressed in this work is only one among many effects one can expect within mesoporous supports. An in-depth study of all these effects might open new applications to this class of materials.

Acknowledgments

This research was supported by the French Ministry of National Education. We thank C. Marcilly and M.

Thomas (IFP) for helpful discussions and P. Beaunier (LRS) for TEM measurements.

References

[1] A.Y. Khodakov, A. Griboval-Constant, R. Bechara and V.L. Zholobenko, J. Catal. 206 (2002) 230.
[2] L. Liz Marzan and A.P. Philipse, Colloids Surf. A 90 (1994) 95.
[3] H. Zhang, Y. Zhang and C. Li, J. Catal. 238 (2006) 369.
[4] M.D. Jones, R. Raja, J.M. Thomas, B.F.G. Johnson, D.W. Lewis, J. Rouzaud and K.D.M. Harris, Angew. Chem. Int. Edit. 42 (2003) 4326.
[5] R. Raja, J.M. Thomas, M.D. Jones, B.F.G. Johnson and D.E.W. Vaughan, J. Am. Chem. Soc. 125 (2003) 14982.
[6] H.M. Hultman, M. de Lang, M. Nowotny, I.W.C.E. Arends, U. Hanefeld, R.A. Sheldon and T. Maschmeyer, J. Catal. 217 (2003) 264.
[7] H.M. Hultman, M. de Lang, I.W.C.E. Arends, U. Hanefeld, R.A. Sheldon and T. Maschmeyer, J. Catal. 217 (2003) 275.
[8] S. Xiang, Y. Zhang, Q. Xin and C. Li, Chem. Commun. (2002) 2696.
[9] K.I. Zamaraev and J.M. Thomas, Adv. Catal. 41 (1996) 335.
[10] C.M. Zicovich-Wilson, A. Corma and P. Viruela, J. Phys. Chem. 98 (1994) 10863.
[11] L.Z. Zhang, P. Cheng and D.Z. Liao, J. Chem. Phys. 117 (2002) 5959.
[12] N.M. Ostrovski and N.M. Bukhavtsova, React. Kinet. Catal. Lett. 56 (1995) 391.
[13] N.M. Bukhavtsova and N.M. Ostrovskii, React. Kinet. Catal. Lett. 65 (1998) 321.
[14] N.M. Ostrovskii, N.M. Bukhavtsova and V.K. Duplyakin, React. Kinet. Catal. Lett. 53 (1994) 253.
[15] P. Trens, N. Tanchoux, P.-M. Papineschi, D. Maldonado, F. di Renzo and F. Fajula, Micropor. Mesopor. Mater. 86 (2005) 354.
[16] E.G. Derouane and C.D. Chang, Micropor. Mesopor. Mater. 35–36 (2000) 425.
[17] E.G. Derouane, J. Mol. Catal. A: Chem. 134 (1998) 29.
[18] Y. Gao, L.D. Kispert, T.A. Konovalova and J.N. Lawrence, J. Phys. Chem. B 108 (2004) 9456.
[19] J.M. Kim, S. Jun and R. Ryoo, J. Phys. Chem. B 103 (1999) 6200.
[20] A. Sampieri, S. Pronier, J. Blanchard, M. Breysse, S. Brunet, K. Fajerwerg, C. Louis and G. Perot, Catal. Today 107–108 (2005) 537.
[21] R.D. Gonzalez and H. Miura, Catal. Rev. Sci. Eng. 36 (1994) 145.
[22] P. Tian, J. Blanchard, K. Fajerwerg, M. Breysse, M. Vrinat and Z. Liu, Micropor. Mesopor. Mater. 60 (2003) 197–206.
[23] B. Zhu, F. Letellier, J. Blanchard, K. Fajerwerg, C. Louis, D. Guillaume, D. Uzio and M. Breysse, Stud. Surf. Sci. Catal. (submitted).
[24] M. Kruk, M. Jaroniec and A. Sayari, Chem. Mater. 11 (1999) 492.
[25] G. Bergeret, P. Gallezot, in: *Handbook of Heterogeneous Catalysis*, eds. G. Ertl, H. Knözinger and J. Weitkamp (Wiley VCH, Weinheim, 1997).
[26] A.K. Neyestanaki, H. Backman, P. Maki-Arvela, J. Warna, T. Salmi and D.Y. Murzin, Chem. Eng. J. 91 (2003) 271.
[27] P.B. Weisz and C.D. Prater, Adv. Catal. 6 (1954) 143.
[28] J.F. LePage (Paris, Technip, 1978).
[29] C.N. Satterfield (MIT Press, Cambridge, Massachusetts, 1970).
[30] C. N. Satterfield (McGraw-Hill Book Company, New-York, 1980).
[31] R. Gomez, G. Del Angel, C. Damian and G. Corro, React. Kinet. Catal. Lett. 11 (1979) 137.
[32] M. Viniegra, G. Cordoba and R. Gomez, J. Mol. Catal. 58 (1990) 107.
[33] R. Melendrez, A. Alarcon, G. Del Angel and R. Gomez, React. Kinet. Catal. Lett. 70 (2000) 113.
[34] E. Guillon, J. Lynch, D. Uzio and B. Didillon, Catal. Today 65 (2001) 201.
[35] Y. Inoue, J.M. Herrmann, H. Schmidt, R.L. Burwell Jr., J.B. Butt and J.B. Cohen, J. Catal. 53 (1978) 401.
[36] A. Kalantar Neyestanaki, P. Maki-Arvela, H. Backman, H. Karhu, T. Salmi, J. Vayrynen and D.Y. Murzin, J. Catal. 218 (2003) 267.
[37] H. Backman, A.K. Neyestanaki and D.Y. Murzin, J. Catal. 233 (2005) 109.
[38] M.A. Keane, J. Catal. 166 (1997) 347.
[39] S. Smeds, D. Murzin and T. Salmi, Appl. Catal. A: General 150 (1997) 115.
[40] D. Murzin, S. Smeds and T. Salmi, React. Kinet. Catal. Lett. 60 (1997) 57.
[41] M. Kruk, M. Jaroniec and A. Sayari, J. Phys. Chem. B 101 (1997) 583.
[42] A. Zhao and B.C. Gates, J. Catal. 168 (1997) 60.